



Cite this: *Energy Adv.*, 2023, 2, 420

## Early stage techno-economic and environmental analysis of aluminium batteries†

Niklas Lindahl<sup>ab</sup> and Patrik Johansson<sup>cd</sup> 

For any proper evaluation of next generation energy storage systems technological, economic, and environmental performance metrics should be considered. Here conceptual cells and systems are designed for different aluminium battery (AlB) concepts, including both active and passive materials. Despite the fact that all AlBs use high-capacity metal anodes and materials with low cost and environmental impact, their energy densities differ vastly and only a few concepts become competitive taking all aspects into account. Notably, AlBs with high-performance inorganic cathodes have the potential to exhibit superior technological and environmental performance, should they be more reversible and energy efficient, while at the system level costs become comparable or slightly higher than for both AlBs with organic cathodes and lithium-ion batteries (LIBs). Overall, with continued development, AlBs should be able to complement LIBs, especially in light of their significantly lower demand for scarce materials.

Received 18th September 2022,  
Accepted 26th January 2023

DOI: 10.1039/d2ya00253a

rsc.li/energy-advances

## Introduction

The ongoing transition to low-carbon energy systems is characterized by increasing amounts of renewable wind and solar power, leading to variability in sourcing, and thus requires flexible solutions.<sup>1,2</sup> Energy storage provides flexibility, not least rechargeable battery energy storage systems (BESSs) with reversible conversion of electrical to chemical energy at very high roundtrip efficiency, most often *ca.* 90% at the system level.<sup>3</sup> Today, rechargeable batteries, in particular lithium-ion batteries (LIBs), are applied in a large range of applications, from portable electronics and electric vehicles (EVs) to utility-scale BESSs.<sup>4,5</sup> For mobile applications, energy density and charging time are the most important key performance indicators (KPIs) (in addition to the omni-important safety aspects), while for stationary applications, storage lifetime and cost are more important. For stationary BESSs used in energy arbitrage this translates *e.g.* to the KPIs for 2030 of a specific energy density of 250 W h kg<sup>-1</sup> for 15 000 cycles at capital expenditures (CAPEX) of 0.03 € per kW h per cycle (system level).<sup>6</sup> These are in stark contrast to the KPIs for EV application of 450 W h kg<sup>-1</sup> for 2000 cycles and a CAPEX of 85 € per kW h at the pack

level – rendering 0.04 € per kW h per cycle.<sup>6</sup> Furthermore, most stakeholders in utility energy storage consider the environmental impact to be of equal importance to the economic performance and more important than the technological performance.<sup>3</sup>

One battery chemistry, amongst the many next generation battery (NGB) chemistries being put forward at present to replace or complement today's LIBs,<sup>7,8</sup> that is suitable to reach the KPIs for BESSs is aluminium batteries (AlBs).<sup>8–12</sup> The main reasons are their fundamental promise of high capacities and energy densities, from the use of multivalent Al<sup>3+</sup> ions and thus up to 3-electron transfer per cation; the very high capacity (2981 mA h g<sup>-1</sup>) of Al metal anodes; and, especially important for BESS applications, the base being abundant and low-cost materials. On the drawback side, the large amount of energy required to make Al metal naturally comes in, but the well-established highly efficient recycling schemes can largely compensate.<sup>9</sup> Also, as for more battery specific properties, all AlBs are significantly limited by the rather high reduction potential of Al (−1.66 V vs. SHE), thus *ca.* 1.4 V above that of Li (−3.04 V vs. SHE), making it more difficult to create high-voltage cells. Yet, there are many conceptually different designs of AlBs originating from this common baseline, foremost with respect to the different types of cathodes employed *e.g.* graphitic, organic, or inorganic (Fig. 1(A)–(C)).

One intrinsic and common problem is the high charge/radius ratio of the Al<sup>3+</sup> ion, which raises problems in finding electrolyte and cathode combinations allowing for both reversibility and high energy density. The most common electrolytes for AlBs are based on ionic liquids (ILs) that create Al<sub>2</sub>Cl<sub>7</sub><sup>−</sup> and AlCl<sub>4</sub><sup>−</sup> anions.<sup>10,12</sup> The latter anions are intercalated when

<sup>a</sup> Department of Physics, Gothenburg University, SE-412 96 Göteborg, Sweden

<sup>b</sup> Energy Conversion, Research Institutes of Sweden, SE-504 62, Borås, Sweden

<sup>c</sup> Department of Physics, Chalmers University of Technology, SE-412 96 Göteborg, Sweden. E-mail: patrik.johansson@chalmers.se

<sup>d</sup> ALISTORE-European Research Institute, CNRS FR 3104, Hub de l'Energie, Rue Baudelocque, 80039 Amiens Cedex, France

† Electronic supplementary information (ESI) available: Spreadsheets with calculations made. See DOI: <https://doi.org/10.1039/d2ya00253a>



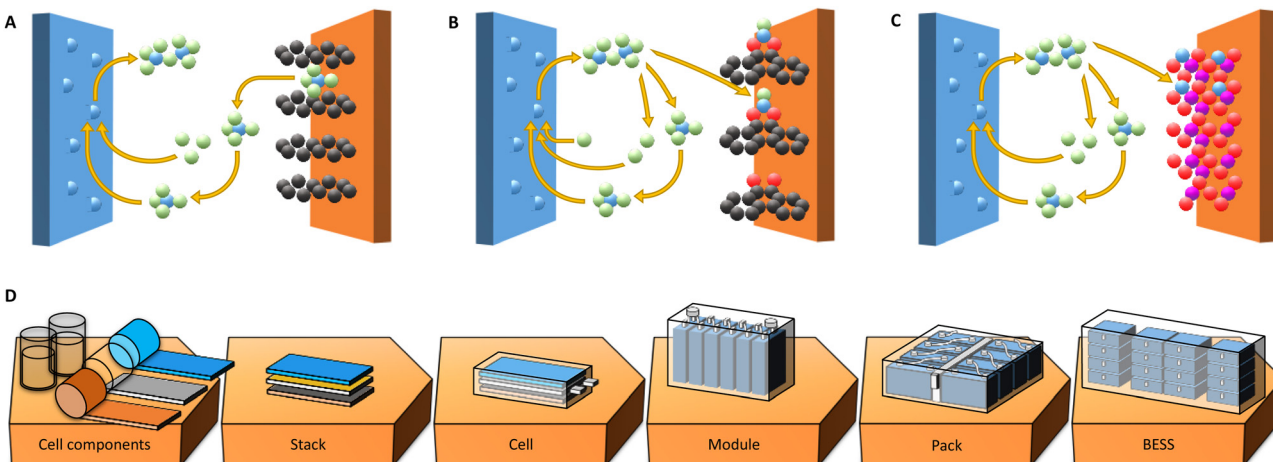


**Fig. 1** Different AlB concepts and the path from cell components to BESSs. (A)–(C) Schematic reactions for the involved species composed of Al (blue) and Cl (green) atoms during discharge for the different AlB concepts with graphite (A), organic (B), and inorganic cathodes (C). (D) The common path from cell components (powders for cathode slurry, electrolyte, Al anode foil, separator, and current collector foil); via assembly into stacks, cells, modules, and packs; and finally into a BESS.

employing graphitic cathodes (Fig. 1(A)) and extracted from the electrolyte.<sup>13,14</sup> Thus, using such cathodes the AlB energy density is fundamentally limited by the volume of electrolyte needed, which in turn depends on the density of ions in the electrolyte, rendering specific cell energy densities of no more than *ca.* 70 W h kg<sup>-1</sup>.<sup>14</sup>

Another approach is to employ the same type of electrolytes and organic cathodes, with redox centers of for example carbonyl groups, such as in quinones, where typically either  $\text{AlCl}^{2+}$  or  $\text{AlCl}_2^+$  cations, rather than  $\text{Al}^{3+}$  cations, are made to coordinate (Fig. 1(B)).<sup>15,16</sup> None of these three cations, however, are thermodynamically stable in the bulk of the electrolyte; they are formed by the dissociation of  $\text{Al}_2\text{Cl}_7^-$  close to the cathode surface.<sup>7,17</sup> Since the coordinated cations are both Cl-containing, the AlB concept using organic cathodes also derives its capacity partly from, and is likewise limited by, the electrolyte. A notable difference is that when employing  $\text{AlCl}^{2+}$  cations the amount of electrolyte required to store the same amount of charge as when using  $\text{AlCl}_4^-$  anions is fundamentally only 1/8.<sup>18,19</sup> Indeed, higher specific energy densities have already been demonstrated and are envisaged to be able to reach *ca.* 200 W h kg<sup>-1</sup>.<sup>19,20</sup>

Finally, cathodes able to truly intercalate  $\text{Al}^{3+}$  cations, in a similar fashion to traditional inorganic cathodes employed in LIBs (Fig. 1(C)), would in principle endow AlBs with even higher energy densities. This is because they would not depend on the electrolyte in at all the same way. As of today, cathodes based on *e.g.* Mo, V, or Ti as the active transition metals have together with IL based electrolytes provided specific cell energy densities of 60–120 W h kg<sup>-1</sup>,<sup>21–23</sup> while inorganic cathodes based on V or Mn and aqueous electrolytes have yielded *ca.* 225<sup>24</sup> and 370<sup>25–27</sup> W h kg<sup>-1</sup>, respectively. Although this may sound remarkable, the (very) strong interactions between the  $\text{Al}^{3+}$  ions and the cathode hosts result in high charging over-potentials and hence low energy efficiencies of *ca.* 40% and 70% for  $\text{TiO}_2$

and  $\text{MnO}_2$ ,<sup>23,27</sup> respectively, compared to *ca.* 90% for AlBs with graphite or organic cathodes.<sup>14,20</sup> Furthermore, these kinds of cells employing aqueous electrolytes have not yet demonstrated fully reversible stripping/plating of Al.<sup>28,29</sup>

For any NGB technology, prospective analyses of practical performance can reveal benefits and limitations, especially if the full chain from cell components to assembly for application and subsequent integration can be covered (Fig. 1(D)) and each level explicitly considered. While AlBs are at a very early stage of development and therefore practical cells are still lacking, they can be expected to be similar to LIBs at the manufacturing and assembly stages and levels.<sup>7,30,31</sup> Hence, conceptual cells, taking into account the specific possibilities and limitations of the different concepts (Fig. 1(A)–(C)), can be modelled and provide essential information. This has indeed been done before for both LIBs and NGBs, although not for AlBs, through creating balanced cell stacks by a bottom-up approach including properties of both active and passive materials.<sup>32,33</sup> One particularly significant difference as compared to LIBs is clearly the importance of the electrolyte and separator properties for those AlB concepts (Fig. 1(A) and (B)) where the electrolyte contributes actively to the cell energy density.<sup>33,34</sup>

Herein the generic path (Fig. 1(D)) from a single cell and its components to multiple-layer stacked cells, *via* putting modules into a battery pack, and finally to a BESS integrated in a container is followed.<sup>5,35</sup> This is made not only for performance related KPIs, but also for monetary KPIs – hence enabling techno-economic modelling and analysis. The BatPaC software<sup>36</sup> has been instrumental for this kind of analysis of cells and packs of commercial LIBs for EV application and has recently also been applied to NGBs.<sup>4,8</sup> Here we apply this procedure to the three different AlB concepts, taking care to properly design and balance the cells, and benchmark them *vs.* several different LIB cells and storage solutions, that are all constructed in the same way.



For the corresponding environmental performance, life cycle analyses (LCAs) have been made bottom-up from materials at the cell level for several LIB chemistries applied in EVs,<sup>37</sup> but indeed also for AlBs based on graphite cathodes.<sup>38</sup> At the utility-scale, *i.e.* the BESS level, however, most studies of environmental impact have been based on commercially available modules, and this limits the possibilities to evaluate NGBs, as much of the input needed is not available. Therefore, we here choose a more accessible alternative; the long-term availability in the Earth's crust of the elements used, *via* the crustal scarcity potential (CSP).<sup>39</sup> While this does not take into account any specific routes of production *etc.*, it is at the same time not laden with the large uncertainties as large assumptions of such routes would introduce. To this we also add a minor global warming potential (GWP) analysis.

All of the above, from materials and conceptual cell design to utility-scale BESSs, is made as transparent as possible and all relevant data are outlined in a spreadsheet.

## Results

### Technical performance

Systematic calculations of the amounts of various materials employed and the practically achievable energy densities were performed for several AlBs with cathodes of graphite (**Al-gra**); organic compounds, poly(phenanthrenequinone) (**Al-PPQ**) and poly(benzoquinonyl sulfide) (**Al-PBQS**); and inorganic hosts, titanium dioxide (**Al-TiO<sub>2</sub>**), potassium-vanadium pentoxide (**Al-KV<sub>2</sub>O<sub>5</sub>**), and manganese dioxide (**Al-MnO<sub>2</sub>**). In addition, LIBs with anodes of graphite and cathodes of lithium nickel-manganese-cobalt oxide (**LIB-NMC**), more specifically NMC811-based, and lithium iron phosphate (**LIB-LFP**), were created as well as a dual-ion battery based on two graphite electrodes (**Li-DIB**).

Starting at the material level and cell designs, we first consider only the properties of the active materials (AM) used in the different concepts, wherefrom some very ideal and theoretical "cell" energy densities can be obtained (Table 1). Please note that for the cells based on graphitic (**Al-gra** and **Li-DIB**) and organic (**Al-PPQ** and **Al-PBQS**) cathodes the

electrolyte needed must be taken into account. Hence, the exceptional capacity of the Al metal anode cannot be used single-handedly as a measure for the promise of all AlB cells, as should be clear by comparing columns 1 and 2 *vs.* columns 3 and 4 in Table 1. This process overall follows that often used to promote various NGBs (as well as novel materials for LIBs), but which is often also laden with many problems, not least transparency with respect to comparisons with commercial batteries.<sup>30,33,40</sup>

The **Al-PPQ** and **Al-PBQS** cells are based on cathode materials with fair and high specific capacities, but as these have comparatively low volumetric capacities, due to the common feature of low density of organic compounds, the cells have rather low volumetric energy densities. The **Al-gra** cell, due to the larger electrolyte demand, is less than half as energy dense both gravimetrically and volumetrically. In contrast, the lower specific capacity and cell voltage of **TiO<sub>2</sub>** are "compensated" for by the Al metal anode utilization and the higher densities of inorganic materials provide the **Al-TiO<sub>2</sub>** cells almost similar volumetric energy densities to the **Al-PBQS** cells, which is *ca.* half that of **Al-KV<sub>2</sub>O<sub>5</sub>** and 4 times lower than that for the **Al-MnO<sub>2</sub>** cells. If the latter AlB concept can overcome its energy efficiency problems, all other things being equal, it would be outstanding and even match **LIB-NMC** in terms of energy density, albeit at a much lower cell voltage.

Thus, when estimating the cell energy densities that are practically obtainable, including electrolyte and passive materials, a slightly different picture emerges than when only looking at the anode and cathode materials. The cell design also deeply depends on the intended application, not least the energy/power performance needed. Here, the intended BESS application is energy arbitrage with daily charge and discharge for 4 h and therefore relatively thick electrodes of up to 200  $\mu\text{m}$  are used.<sup>36,41</sup> From this, the thicknesses of all other components are deduced (Fig. 1(D), Methods).

The high volumetric capacity of Al, and that it is used both as an anode and a current collector (CC) in combination, gives *ca.* 30% thinner single-cell stacks for AlBs than for LIBs (Fig. 2(A)). However, for **Al-gra** this advantage is lost by the very thick separator needed, and the same is true, to a somewhat lesser extent, for **Li-DIBs**.<sup>34</sup> Furthermore, the graphite expansion requires extra volume in the stack design for both LIBs and

Table 1 Properties of the active materials, including the electrolyte needed, and the cells 'created'

Concept	Anode		Anode and electrolyte		Cathode		Cell		
	Specific capacity	Volumetric capacity	Specific capacity	Volumetric capacity	Specific capacity	Volumetric capacity	Average voltage	Specific energy density	Volumetric energy density
	[mA h g <sup>-1</sup> ]	[mA h cm <sup>-3</sup> ]	[mA h g <sup>-1</sup> ]	[mA h cm <sup>-3</sup> ]	[mA hg <sup>-1</sup> ]	[mA h cm <sup>-3</sup> ]	[V]	[W h kg <sup>-1</sup> ]	[W h L <sup>-1</sup> ]
Al-gra	2981	8049	49	58	135	297	2.00	72	98
Al-PPQ	2981	8049	344	413	170	272	1.40	159	230
Al-PBQS	2981	8049	344	413	300	480	1.60	257	355
Al-TiO <sub>2</sub>	2981	8049	2981	8049	110	465	0.64	68	282
Al-KV <sub>2</sub> O <sub>5</sub>	2981	8049	2981	8049	225	716	1.00	209	657
Al-MnO <sub>2</sub>	2981	8049	2981	8049	285	1428	1.30	338	1577
LIB-NMC	372	818	372	818	210	977	3.65	490	1625
LIB-LFP	372	818	372	818	160	584	3.30	369	1125
Li-DIB	372	818	77	107	140	308	4.50	223	358



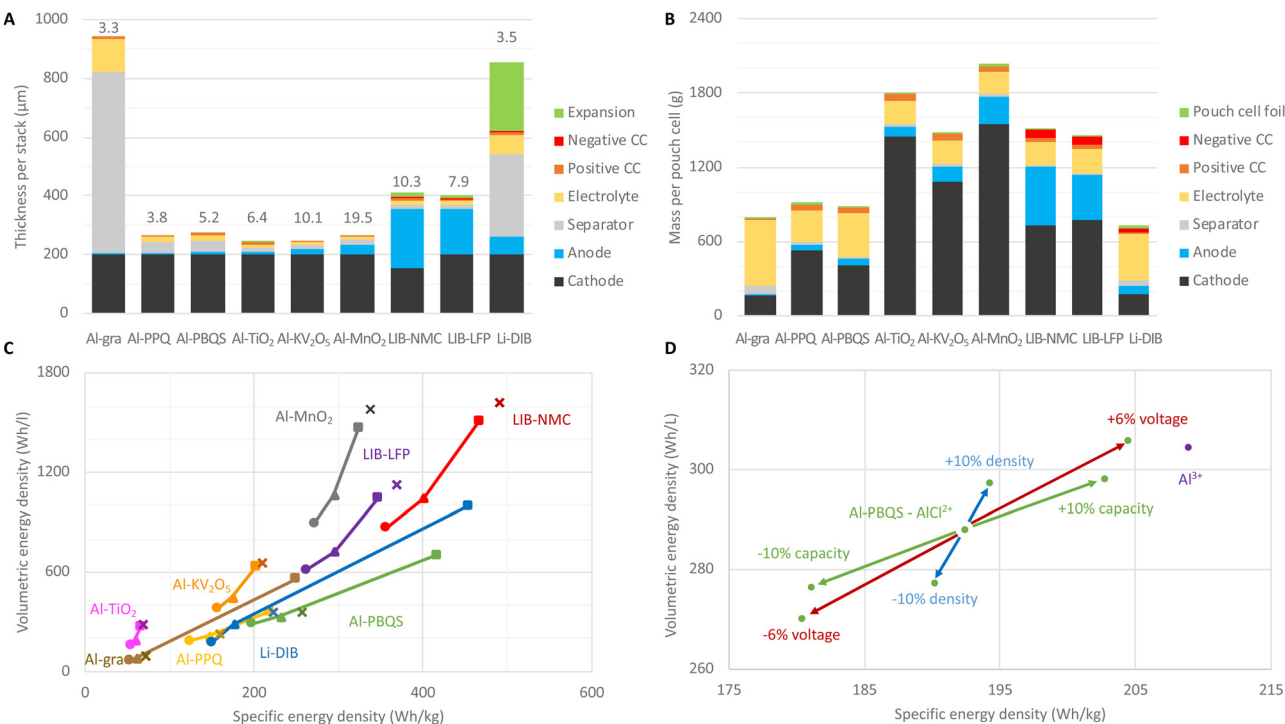


**Fig. 2** Cell designs and technical performance. (A) Thicknesses per stack. The numbers above the bars are the areal capacities ( $\text{mA h cm}^{-2}$ ). (B) Masses per pouch cell. (C) Volumetric vs. specific energy density at different steps for conceptual cell designs. Step 1 (squares) considers only active materials. Step 2 (triangles) considers electrodes and the electrolyte required in practical cells. Step 3 (circles) considers all active and passive materials needed to create practical cells. Theoretical “cells” (crosses) consider active materials and the minimum need for electrolyte. (D) Sensitivity analysis for the energy densities of Al-PBQS at the cell level.

**Li-DIBs**, but for **Al-gra** the 80% cathode expansion<sup>42</sup> is more than compensated for by the 33% electrolyte volume decrease.<sup>43</sup> The areal capacity is dependent upon and limited by the volumetric capacity and, hence, cells with inorganic cathodes come out better.

The material masses in a pouch cell (Fig. 2(B)) depend on the layer thicknesses in the stack, the number of stacks that fit into the cell, and the materials’ densities. The high densities of the inorganic cathode active materials lead to both larger masses per cell for these AlBs and a larger percentage of the total cell masses (*ca.* 75%) than for both AlBs with organic cathodes and LIBs (*ca.* 50%) as well as for **Al-gra** and **Li-DIBs** (*ca.* 25%). Thus, the relative reduction from theoretical to practical specific capacity is less prominent for the former AlB concept.

Overall, the evolution of the energy densities (Fig. 2(C)) from only electrode active materials (step 1, squares), *via* the making of electrodes and introducing the electrolyte (step 2, triangles), to practical cells (step 3, circles) shows that the losses between steps 1 and 2 are more pronounced for the cell concepts requiring larger electrolyte amounts. The loss in volumetric energy density between steps 1 and 3 is *e.g.*  $>80\%$  for the **Al-gra** and **Li-DIB** cell designs. However, the loss of *ca.* 50% is similar for **Al-PPQ**, while only slightly higher for **Al-PBQS** (60%) and correspondingly slightly lower for AlBs and LIBs with inorganic cathodes (*ca.* 40%). This is largely due to the fact that the volume of electrolyte, needed in practical cells to fill the porous electrodes, is similar. Hence, the theoretical estimates

(Fig. 2(C), crosses, and Table 1, columns 8 and 9) are closer to step 2 for the concepts using graphitic or organic cathodes, but closer to step 1 for those with inorganic cathodes.

A comparison between the best performing AlBs reveals that, at the cell level, **Al-PBQS** has *ca.* 75% of the specific energy density but only *ca.* 1/3 of the volumetric energy density of **Al-MnO<sub>2</sub>**. For the **Al-PBQS** cell (Fig. 2(D)) an increase in density or capacity of the organic cathode by 10% only increases the volumetric energy density by *ca.* 3%. This is because the increased capacities also require larger volumes of electrolyte. If the reaction mechanism could be changed to involve  $\text{Al}^{3+}$  instead of  $\text{AlCl}^{2+}$  the increase in volumetric energy density would still only be *ca.* 6%, as an electrolyte is needed to fill the pores. However, if it employed  $\text{AlCl}_2^+$  the volumetric energy density would be *reduced* by more than 60% (not shown), which stresses the importance of an accurate determination of the reaction mechanism.<sup>12</sup>

### Economic performance

The use of low-cost materials often gives rise to claims of AlBs being inherently low cost, but the relevant metric is cost per unit of (useable) energy stored. Applying this measure, first at the cell level, the **Al-PBQS** and **Al-MnO<sub>2</sub>** cells achieve *ca.* 25 \$ per kW h, and **LIB-NMC** and **LIB-LFP** have *ca.* 150 and 100% higher cost, respectively, whereas **Al-gra** has a vast cost of *ca.* 120 \$ per kW h (Fig. 3(A)). Both of the other inorganic cathode-based AlBs come out as relatively expensive, despite

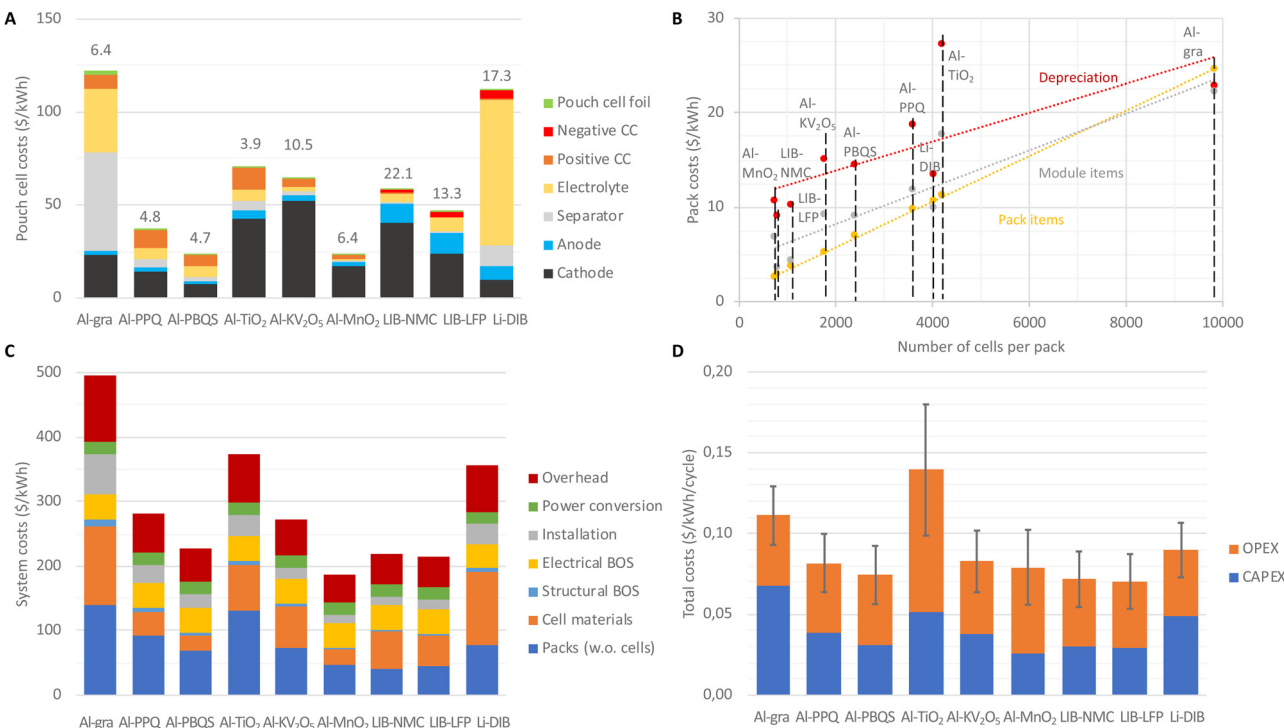


**Fig. 3** Economic performance from the cell to BESS level. (A) Material costs at the cell level. The numbers above the bars are the costs per mass (\$ per kg). (B) Breakdown of costs at the pack level. The dotted lines are linear fits. (C) Costs at the utility-scale BESS level. (D) Total costs of a utility-scale BESS. The error bars are sensitivity to an average cost of electricity varying between 0.02 and 0.04 \$ per kWh.

the low material costs for **Al-TiO<sub>2</sub>**. As compared to the literature, our costs are similar for **Al-gra**<sup>11</sup> and slightly lower for **LIB-NMC**, much due to our cell being designed with a thicker cathode.<sup>5,41</sup> Breaking down the costs (Fig. 3(A)), the inorganic cathodes make up a large majority (70–90%) of the material costs for those AlB cells (with a notable exception for **Al-TiO<sub>2</sub>**), but the cathode cost is much less for other AlB cells, *e.g.* 30% for **Al-PBQS**. The latter renders the cost of the passive materials relatively more important. Admittedly, there is a need for a caveat here; whereas the costs for materials in LIBs are based on commercial cell costs,<sup>36</sup> and therefore rather trustworthy even if volatile, some materials used for the AlBs, *e.g.* the IL based electrolyte and the organic cathodes, are rather unique and their costs in large quantities are therefore laden with much larger uncertainties. Although these are relatively important at the cell level, where they contribute *ca.* half of the costs, as described below, at the system level their contribution is significantly smaller. Hence, any deviations, both positive and negative, *e.g.* as compared to cathode material costs for inorganic LIBs, would have a relatively limited impact overall.

Moving to battery-packs and utility-scale BESSs (Fig. 3(B)–(D)) renders another set of pictures compared to that solely based on the cells. The higher volumetric energy densities of cells based on inorganic cathodes provide cost benefits; as in the pack-design the cost in general decreases with fewer cells needed (Fig. 3(B)). In more detail, for pack items the costs are mainly due to the battery jacket, which scales with the outer area of the pack, while for module items, the cost is dominated by state-of-charge-controllers needed for each group of cells

connected in parallel. Overall the lower cell voltages of any AlB, as compared to LIBs, result in more cells in series in order to reach the desired pack-voltage and thus more module items are needed.

Looking at different AlB designs and production aspects, the lower areal capacity of organic cathodes as compared to the inorganic cathodes (Fig. 2(A)) means that a larger number of electrodes are required to reach the same pack-energy. For a fixed rate of electrode production, a larger plant is needed and therefore also increased costs for depreciation of manufacturing equipment. Similarly, the low specific energies of **Al-gra**, **Al-TiO<sub>2</sub>**, and **Al-V<sub>2</sub>C** require larger masses of battery materials and, hence, more equipment and higher cost for depreciation.

Finally, the volumetric energy density at the pack-level determines the amount of energy stored in each container and thereby the number of containers needed to create the BESSs for a given energy. Again, cells based on inorganic cathodes obtain cost advantages, as the costs for the structural balance of system (BOS) and installation and thereby overheads are reduced (Fig. 3(C)). In the end, the complete BESS costs become *ca.* 220 \$ per kWh for both the **Al-PBQS** and the LIB concepts, despite the cell materials making up 11% for the former and 27% for **LIB-NMC**.

For the application of daily energy arbitrage, over the assumed lifetime (20 years and *ca.* 7300 cycles), the capital expenditure (CAPEX) for the BESSs reaches the KPI for the **Al-PBQS**, **Al-MnO<sub>2</sub>**, and LIB based solutions (Fig. 3(D)). However, the lower efficiencies of the AlB concepts based on inorganic



cathodes lead to higher operational expenditures (OPEX), mainly governed by the higher cost associated with the electricity used to charge them, which thus depends on the average electricity price – here set to a modest value of  $0.03 \pm 0.01$  \$ per kW h. Therefore total costs (CAPEX + OPEX) are the lowest for the **Al-PBQS** and **LIB** BESSs at *ca.* 0.07 \$ per kW h per cycle, closely followed by the **Al-PPQ**, **Al-KV<sub>2</sub>O<sub>5</sub>**, and **Al-MnO<sub>2</sub>** BESSs at *ca.* 0.08 \$ per kW h per cycle. This small difference can certainly be turned around depending on the exact chemistry employed and this is especially true for the less mature AlB technology and concepts.

### Environmental performance

Similar to the economic performance analysis above, all environmental performance analysis is performed in relation to the useable energy storage. Both the GWP and the CSPs can show whether using abundant materials, often a claim made for AlBs (and other NGBs), is truly beneficial.

It is shown that at the cell level **Al-gra**, **Al-TiO<sub>2</sub>**, and **Al-KV<sub>2</sub>O<sub>5</sub>** have high GWPs, due to lower specific energies and/or high GWPs per mass (Fig. 4(A)). Overall, the cathodes contribute more than half of the GWP for the concepts based on inorganic cathodes, whereas for AlBs based on organic cathodes the electrolyte and the cell assembly add up to *ca.* 40% of the total GWP, and for **Al-gra** and **Li-DIBs** this even makes up 75%. Compared to the literature, our result for **LIB-NMC** is slightly lower than for similar cells for EVs produced in gigafactories from low carbon energy,<sup>44</sup> again mostly due to our high-energy cell design.

At the BESS level (Fig. 4(B)), the main contributions to the GWPs do come from the cell materials. However, the concepts with lower volumetric energy densities require more housing materials, mainly Al and steel in the larger packs and for the BESS containers. For these concepts the use of recycled Al would provide only marginal reductions of the total GWP at the cell level, but together with the use of low-carbon a reduction of *ca.* 35% at the BESS level can be obtained. Recycling of cell materials could clearly reduce the net GWPs, but yet the benefits are most likely larger for concepts based on more precious materials, *e.g.* **LIB-NMC**, than for concepts based on more abundant materials.<sup>45</sup> Although the minor GWP analysis here enables basic comparisons, detailed LCAs are required for more complete evaluations of the AlB-concepts.

The CSPs present clear advantages for most AlBs (except for **Al-gra** and **Al-KV<sub>2</sub>O<sub>5</sub>**) at the cell level (Fig. 4(C)). For the AlBs based on organic cathodes and even more so for **Al-gra**, the majority of the CSP comes from the Cl in the electrolyte. For the concepts based on inorganic cathodes, some of the metals used (V, Ni, Co, and Li) have an effect that cannot even be offset by the high specific energy of the **LIB-NMC** cells, or for **Al-KV<sub>2</sub>O<sub>5</sub>**. However, the low CSP of Ti renders a sufficiently low CSP per mass for the **Al-TiO<sub>2</sub>** design (Fig. 4(C)) to counter its low specific energy density, and the resulting CSP is almost as low as that for the organic AlBs. Although Li contributes a significant and similar (*ca.* 1800 kg Si eq. per kW h) amount to the CSPs in both LIBs and **Li-DIB**, Ni contributes even more with *ca.* 54% of the CSP for the NMC cathode. Furthermore, for LIBs the negative

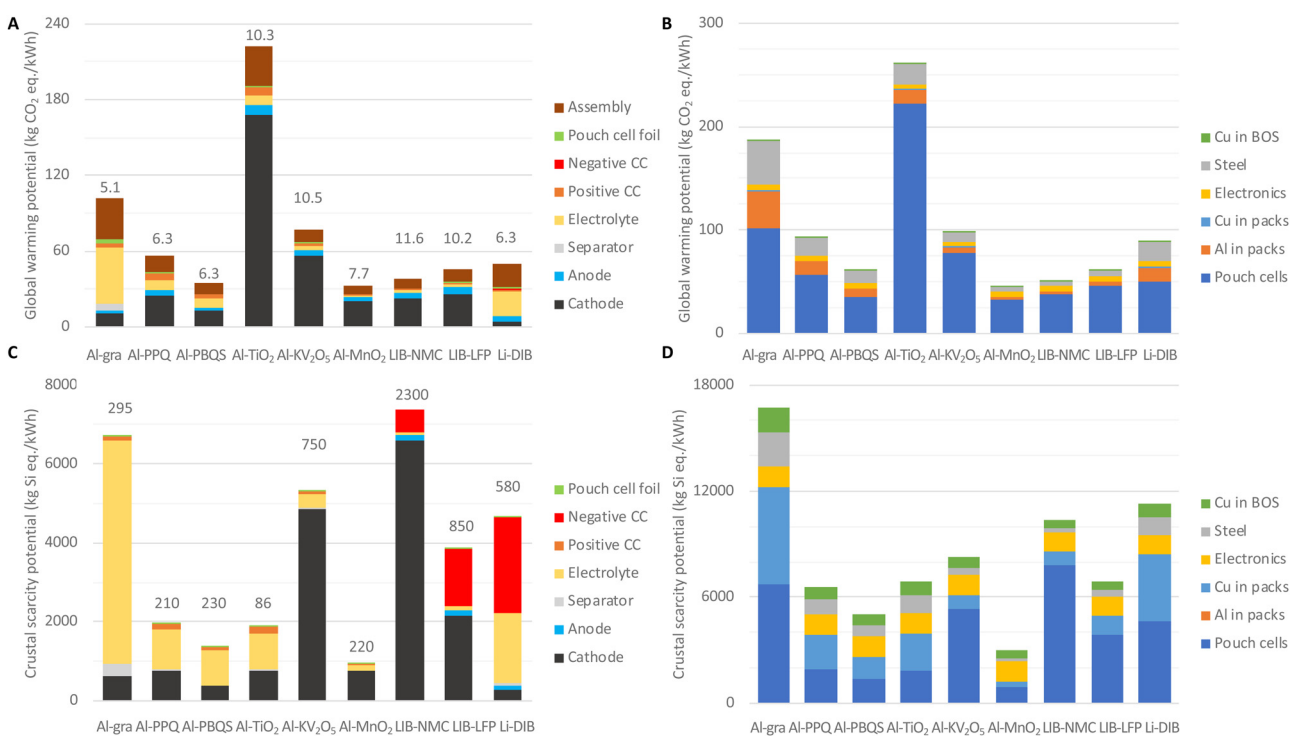


Fig. 4 Environmental performance at cell and BESS levels. (A) GWPs at the cell level. The numbers above the bars are the GWPs per mass (kg CO<sub>2</sub> eq. per kg). (B) GWPs at the utility-scale BESS level. (C) CSPs at the cell level. The numbers above the bars are the CSPs per mass (kg Si eq. per kg). (D) CSPs at the utility-scale BESS level.

CC that has to be made from Cu has a large impact on the total CSP, notably >50% for **Li-DIB** (that anyhow has a rather average total CSP due to the low contribution from graphite electrodes).

At the BESS level (Fig. 4(D)), the concepts with lower volumetric energy densities, thus the same problematic cases as in the economic analysis and for the GWP above, require more wires connecting the larger number of cells inside the pack and BESS containers. Hence, the relative difference in CSPs between AlBs and LIBs becomes smaller when electronics and Cu-wires are also considered. These in fact add up to *ca.* 60% of the CSP for **Al-PPQ**, **Al-PBQS**, **Al-TiO<sub>2</sub>** and **Al-MnO<sub>2</sub>**, but nonetheless, BESSs based on **Al-PBQS** and in particular **Al-MnO<sub>2</sub>** have significantly lower CSPs than any BESS built from LIB cells and packs. As a side-note, the latter **LIB-LFP** reassuringly comes out to be significantly better than **LIB-NMC** and **Li-DIB**.

## Conclusions

In this article, we have evaluated the performance of various AlB concepts based on demonstrated material properties and designs similar to current LIBs. We find that while the low volumetric energy densities hamper **Al-gra**, next generation organic and inorganic AlBs remain promising. The added value of including performance in all most important aspects is stressed; *e.g.* for **Al-TiO<sub>2</sub>** the technical performance is relatively poor, the cell level material cost and CSP are fair, and the system lifetime costs and GWP become prohibitive. Overall, the development of novel materials for AlBs, and for NGBs in general, would thus benefit from including estimates of performance in a broad sense, and if not at a complete system level at least at a cell level looking at cell energy density, materials costs and CSP.

Yet, most experimental AlB-studies use comparatively low areal capacity cathodes and combine these with a large excess

of Al anodes and electrolytes, while optimised electrolyte and electrode loadings are ultimately needed. Lean electrolyte conditions could, however, lead to severely reduced power performance, as observed for **Al-gra**,<sup>46</sup> and the latter could give rise to current densities (for **Al-MnO<sub>2</sub>** *ca.* 5 mA cm<sup>-2</sup>) higher than optimal for the 2D-foil Al-anodes, which could be mitigated by introducing 3D-anodes.<sup>18,47</sup> Furthermore, the cycle-life we assume here has so far only been achieved for **Al-gra**,<sup>13</sup> and fully reversible cell reactions for **Al-MnO<sub>2</sub>** likely require the development of completely novel electrolytes.<sup>28</sup> Overall, *e.g.* Cl-free electrolytes<sup>48</sup> could reduce the CSP by more than half at the cell level, all other things being equal.

Even for the most promising AlB concepts, the excellent performance at the cell level still provides relatively small improvements at the BESS level as compared to LIBs, both in terms of costs and GWPs. Modern cell to pack designs have improved the energy densities at the pack level,<sup>49</sup> and alternative BESS designs optimized for AlBs could similarly provide relative benefits. Combining these there are thus both significant promise and challenges for the various AlB concepts.

The efforts needed to tackle the above challenges are motivated by the promise of AlBs to reach the KPIs for stationary storage by 2030 (Table 2). Although all AlB concepts are based on materials of relatively low cost and environmental impact, these are preferably also to be combined with sufficiently high energy densities, as obtained *e.g.* for **Al-PBQS** and **Al-MnO<sub>2</sub>**. Table 2 shows that while the here considered AlB concepts based on organic cathodes do not meet the KPIs for the energy densities at the cell level, they perform (very) well for the economic KPIs, while the **Al-MnO<sub>2</sub>** AlB both reaches the technological KPIs and has the best CAPEX at the BESS level (but still, at present, falls behind in OPEX due to its lower energy efficiency).

Yet, the main benefit of the AlB concepts will anyhow likely be their low CSPs, lacking appropriate LCAs, indicating not only that AlBs could be more sustainable in long-term than

Table 2 Properties relative to KPIs of the conceptual designs of cells, packs, and BESSs. For GWP and CSP no KPIs exists, why **LIB-LFP** is set = 100%

Concept	Cell level					System level				
	Specific Energy Density [Wh/kg]	Volumetric Energy Density [Wh/L]	Cell Costs [\$/kWh]	GWP [kg CO <sub>2</sub> eq. /kWh]	CSP [kg Si eq. /kWh]	Pack cost [\$/kWh]	CAPEX [\$/kWh /cycle]	OPEX [\$/kWh /cycle]	GWP [kg CO <sub>2</sub> eq. /kWh]	CSP [kg Si eq. /kWh]
KPIs 2030	250	700	70			85	0.03	0.05		
Al-gra	21%	10%	178%	223%	173%	309%	226%	86%	307%	243%
Al-PPQ	49%	26%	55%	124%	50%	152%	129%	86%	152%	96%
Al-PBQS	79%	41%	34%	76%	35%	110%	104%	86%	100%	73%
Al-TiO <sub>2</sub>	22%	23%	103%	485%	48%	238%	170%	177%	428%	101%
Al-KV <sub>2</sub> O <sub>5</sub>	63%	54%	93%	169%	138%	162%	125%	91%	160%	120%
Al-MnO <sub>2</sub>	109%	128%	33%	72%	24%	84%	85%	107%	73%	43%
LIB-NMC	143%	124%	84%	83%	202%	116%	100%	83%	83%	151%
LIB-LFP	105%	87%	67%	46	3871	109%	98%	82%	61	6879
Li-DIB	60%	25%	162%	109%	120%	225%	163%	82%	145%	164%



LIBs, but also that they will be less susceptible to supply shortages during the ongoing and increasing fast growth in demand for energy storage.<sup>4,31</sup> All in all, this implies that AlBs, with either organic or inorganic cathodes, could become a complementary technology to LIBs and readily enable a faster transition to a more sustainable global low-carbon energy system.

## Methods

### Technical performance

The material properties and costs were mainly obtained from BatPaC (version 5.0).<sup>36</sup> The properties of materials needed for the AlBs that are not included in BatPaC should be considered as optimistic, but anyhow realistic estimates, with some continued advancement. The capacity we use for PBQS is based on a similar utilization of the theoretical capacity to that observed for Al-PPQ (*ca.* 70%),<sup>20</sup> and demonstrated in LIBs,<sup>50</sup> but not yet for AlBs.<sup>16</sup> In the cells using inorganic cathode active materials, the electrolyte volume was set by the volume of the pores in electrodes and separator combined, while for AlBs with graphitic or organic cathodes, and for Li-DIB, the electrolyte was set to balance the capacity. For all of the latter cells, the separator thickness was set to provide sufficient pore volume to incorporate the electrolyte needed.<sup>33,34</sup> For each stack, current collectors and the volume needed for electrode expansion are added.

The intended application, daily energy arbitrage with charge (and discharge) in 4 h, means a cell design optimized with respect to energy density, but with lower power density demand, *i.e.* a high E/P number. Here we assume an electrode thickness of 200  $\mu\text{m}$ , which is challenging but possible.<sup>36,41</sup> For the AlBs the anode capacity is at least in 50% surplus, due to the need for the Al metal combined anode and CC to keep its mechanical integrity also when the cell is fully discharged. The AlBs use a cathode CC of 14  $\mu\text{m}$  Al foil coated on both sides with 500 nm of dichromium nitride ( $\text{Cr}_2\text{N}$ ) to prevent corrosion in the Cl-containing IL-based electrolyte.<sup>51</sup> All LIBs use an anode CC of 10  $\mu\text{m}$  Cu foil and a cathode CC of 15  $\mu\text{m}$  Al foil.<sup>36</sup> In the stack assembly, double-coated electrodes are assumed and hence the CC thickness is shared.<sup>32</sup> The pouch cells are 2 cm thick with the anodes set to be 30 cm long and 10 cm wide (and the cathodes 2 mm less in each lateral dimension).

Also at the pack level, BatPaC provided properties and costs of the components.<sup>36</sup> For each cell chemistry, the material properties and module configuration were adjusted to give similar pouch cell sizes and energy densities in the BatPaC-model to those in the conceptual cells. The packs were set to provide *ca.* 960 V and *ca.* 350 kW h usable energy (85% of the installed energy). The BESS modelled is to provide 60 MW during 4 h, *i.e.* 240 MWh usable capacity, and was based on modular 40 ft ISO shipping containers with packs of battery modules together with structural and electronic balance of system (BOS) in addition to the power conversion system (PCS).<sup>52,53</sup> The volume of the battery packs was set to be 35% of the container volume.

### Economic performance

From the materials contents, the materials costs were calculated at the cell-level. The costs of materials in AlBs not included in BatPaC were obtained from other techno-economic analyses: graphite and separators from DIBs;<sup>34</sup> organic cathode materials from disulfonic acid, as a proxy for both PPQ and PBQS;<sup>54</sup> and inorganic cathode materials from various literature sources:  $\text{TiO}_2$ ,<sup>55</sup>  $\text{V}_2\text{O}_5$  as a proxy for  $\text{K}_{0.5}\text{V}_2\text{O}_5$ ,<sup>56</sup> and  $\text{MnO}_2$ .<sup>57</sup> The cost of the IL-based electrolyte was obtained from a cost analysis of Al-gra.<sup>11</sup> The cost of the CC coating was obtained from costs of the thin films of Cr,<sup>58</sup> adjusted for the sputtering conditions for  $\text{Cr}_2\text{N}$ .<sup>51</sup>

BatPaC provides costs for purchased items and non-materials. The latter include costs of depreciation (for a “Giga-factory” producing 100 000 packs *i.e.* *ca.* 40 GWh per year), direct labor, and overheads.<sup>36</sup> Purchased items include *e.g.* cell-interconnects and SOC-controllers in module enclosures assembled into a pack with interconnects and a battery management system (BMS) enclosed in a battery jacket. From the complete costs for the construction of a BESS of 60 MW up to 4 h duration, the costs per MW and per container could be obtained for structural BOS, electrical BOS, installation, PCS, and overheads, respectively.<sup>59</sup> The OPEX was obtained from the costs for daily full charging with electricity at an average cost of 0.03 \$ per kW h, over a life-time of 20 years, for operation and maintenance.<sup>3</sup>

### Environmental performance

From the material contents, the environmental impacts were calculated. The GWP<sub>100</sub> for materials in LIBs and packs were obtained from LCAs performed for LIB-NMC and LIB-LFP.<sup>37,60</sup> The specific GWP<sub>100</sub> for materials exclusively found in AlBs and cell assembly (for both AlBs and LIBs based on renewable electricity only) were obtained from a LCA made for Al-gra.<sup>38</sup> The GWP<sub>100</sub> of cathode materials in AlBs were calculated from LCAs for calix[4]quinone as a proxy for PPQ and PBQS,<sup>61</sup> and for  $\text{TiO}_2$ ,<sup>62</sup>  $\text{V}_2\text{O}_5$  as a proxy for  $\text{K}_{0.5}\text{V}_2\text{O}_5$ ,<sup>56</sup> and  $\text{Mn}_2\text{O}$ .<sup>63</sup> The GWP for the AlB IL-based electrolyte was obtained by combining the GWP<sub>100</sub> for the  $\text{AlCl}_3$  salt and the [EMIM]Cl IL.<sup>64</sup> The GWP of the CC-coating was calculated from LCA for sputtered Cr.<sup>58</sup>

The CSPs for virgin crust elements were used, except for Cl and Cu for which the CSPs were weighted to also account for supplies from other sources, sea-water and recycling, respectively.<sup>39</sup> For the CSP of the electrical BOS and PCS, the electronics were assumed to have the compositions of inverters in EVs.<sup>65</sup>

## Author contributions

Niklas Lindahl: conceptualization, funding acquisition, investigation, methodology, project administration, visualization, writing – original draft; Patrik Johansson: conceptualization, funding acquisition, supervision, writing – review & editing.

## Conflicts of interest

There are no conflicts to declare.

## Acknowledgements

The research reported herein and the report itself have been supported by the Swedish Energy Agency through grants #50121-1 and #43525-1. Our work was significantly improved by the informative discussions with Dr Richard Arvidsson, Chalmers, on environmental impacts; Dr Johan Fridner, Norsk Hydro, on pack level properties; and Dr Jan Eriksson, Hitachi Energy, on system level properties.

## References

- 1 P. D. Lund, J. Lindgren, J. Mikkola and J. Salpakari, *Renewable Sustainable Energy Rev.*, 2015, **45**, 785–807.
- 2 M. S. Ziegler, J. M. Mueller, G. D. Pereira, J. Song, M. Ferrara, Y. M. Chiang and J. E. Trancik, *Joule*, 2019, **3**, 2134–2153.
- 3 M. Baumann, J. Peters and M. Weil, *Energy Technol.*, 2020, **8**, 1901019.
- 4 C. Vaalma, D. Buchholz, M. Weil and S. Passerini, *Nat. Rev. Mater.*, 2018, **3**, 18013.
- 5 R. Schmuck, R. Wagner, G. Hörpel, T. Placke and M. Winter, *Nat. Energy*, 2018, **3**, 267–278.
- 6 Batteries Europe – Strategic Research Agenda for batteries, 2020.
- 7 Y. Liang, H. Dong, D. Aurbach and Y. Yao, *Nat. Energy*, 2020, **5**, 646–656.
- 8 A. Ponrouch, J. Bitenc, R. Dominko, N. Lindahl, P. Johansson and M. R. Palacin, *Energy Storage Mater.*, 2019, **20**, 253–262.
- 9 T. Leisegang, F. Meutzner, M. Zschornak, W. Münchgesang, R. Schmid, T. Nestler, R. A. Eremin, A. A. Kabanov, V. A. Blatov and D. C. Meyer, *Front. Chem.*, 2019, **7**, 268.
- 10 B. Craig, T. Schoetz, A. Cruden and C. Ponce de Leon, *Renewable Sustainable Energy Rev.*, 2020, **133**, 110100.
- 11 G. A. Elia, K. V. Kravchyk, M. V. Kovalenko, J. Chacón, A. Holland and R. G. A. Wills, *J. Power Sources*, 2021, **481**, 228870.
- 12 K. L. Ng, B. Amrithraj and G. Azimi, *Joule*, 2022, **6**, 134–170.
- 13 M.-C. Lin, M. Gong, B. Lu, Y. Wu, D.-Y. Wang, M. Guan, M. Angell, C. Chen, J. Yang, B.-J. Hwang and H. Dai, *Nature*, 2015, **520**, 324–328.
- 14 K. V. Kravchyk, S. Wang, L. Piveteau and M. V. Kovalenko, *Chem. Mater.*, 2017, **29**, 4484–4492.
- 15 D. J. Kim, D. J. Yoo, M. T. Otley, A. Prokofjevs, C. Pezzato, M. Owczarek, S. J. Lee, J. W. Choi and J. F. Stoddart, *Nat. Energy*, 2019, **4**, 51–59.
- 16 J. Bitenc, N. Lindahl, A. Vizintin, M. E. Abdelhamid, R. Dominko and P. Johansson, *Energy Storage Mater.*, 2020, **24**, 379–383.
- 17 D. J. Yoo and J. W. Choi, *J. Phys. Chem. Lett.*, 2020, **11**, 2384–2392.
- 18 N. Lindahl, J. Bitenc, R. Dominko and P. Johansson, *Adv. Funct. Mater.*, 2020, **2004573**, 3–9.
- 19 D. Yoo, M. Heeney, F. Glöcklhofer and J. W. Choi, *Nat. Commun.*, 2021, **12**, 1–9.
- 20 J. Bitenc, U. Košir, A. Vizintin, N. Lindahl, A. Krajnc, K. Pirnat, I. Jerman and R. Dominko, *Energy Mater. Adv.*, 2021, **2021**, 1–9.
- 21 W. Yang, H. Lu, Y. Cao, B. Xu, Y. Deng and W. Cai, *ACS Sustainable Chem. Eng.*, 2019, **7**, 4861–4867.
- 22 A. Vahidmohammadi, A. Hadjikhani, S. Shahbazmohamadi and M. Beidaghi, *ACS Nano*, 2017, **11**, 11135–11144.
- 23 S. Wang, K. V. Kravchyk, S. Pigeot-Rémy, W. Tang, F. Krumeich, M. Wörle, M. I. Bodnarchuk, S. Cassaignon, O. Durupthy, S. Zhao, C. Sanchez and M. V. Kovalenko, *ACS Appl. Nano Mater.*, 2019, **2**, 6428–6435.
- 24 X. Li, Y. Tang, C. Li, H. Lv, H. Fan, W. Wang, T. Cai, Y. Cui, W. Xing, Z. Yan, C. Zhi and H. Li, *J. Mater. Chem. A*, 2022, **10**, 4739–4748.
- 25 C. Wu, S. Gu, Q. Zhang, Y. Bai, M. Li, Y. Yuan, H. Wang, X. Liu, Y. Yuan, N. Zhu, F. Wu, H. Li, L. Gu and J. Lu, *Nat. Commun.*, 2019, **10**, 73.
- 26 S. He, J. Wang, X. Zhang, J. Chen, Z. Wang, T. Yang, Z. Liu, Y. Liang, B. Wang, S. Liu, L. Zhang, J. Huang, J. Huang, L. A. O'Dell and H. Yu, *Adv. Funct. Mater.*, 2019, **29**, 1905228.
- 27 W. Pan, J. Mao, Y. Wang, X. Zhao, K. W. Leong, S. Luo, Y. Chen and D. Y. C. Leung, *Small Methods*, 2021, **5**, 2100491.
- 28 T. Dong, K. L. Ng, Y. Wang, O. Voznyy and G. Azimi, *Adv. Energy Mater.*, 2021, **11**, 2100077.
- 29 G. Pastel, Y. Chen, T. P. Pollard, M. A. Schroeder, M. E. Bowden, A. Zheng, N. T. Hahn, L. Ma, V. Murugesan, J. Ho, M. Garaga, O. A. Borodin, K. T. Mueller, S. G. Greenbaum and K. Xu, *Energy Environ. Sci.*, 2022, **15**, 2460–2469.
- 30 E. Faegh, B. Ng, D. Hayman and W. E. Mustain, *Nat. Energy*, 2021, **6**, 21–29.
- 31 F. Duffner, N. Kronemeyer, J. Tübke, J. Leker, M. Winter and R. Schmuck, *Nat. Energy*, 2021, **6**, 123–134.
- 32 E. J. Berg, C. Villevieille, D. Streich, S. Trabesinger and P. Novák, *J. Electrochem. Soc.*, 2015, **162**, A2468–A2475.
- 33 J. Betz, G. Bieker, P. Meister, T. Placke, M. Winter and R. Schmuck, *Adv. Energy Mater.*, 2019, **9**, 1803170.
- 34 T. Placke, A. Heckmann, R. Schmuck, P. Meister, K. Beltrop and M. Winter, *Joule*, 2018, **2**, 2528–2550.
- 35 A. Kwade, W. Haselrieder, R. Leithoff, A. Modlinger, F. Dietrich and K. Droeder, *Nat. Energy*, 2018, **3**, 290–300.
- 36 P. Nelson, K. Gallagher, I. Bloom and D. Dees, BatPac v5.0, 2022, <https://www.anl.gov/cse/batpac-model-software>.
- 37 Q. Dai, J. C. Kelly, L. Gaines and M. Wang, *Batteries*, 2019, **5**, 48.
- 38 M. A. S. Delgado, L. Usai, L. A. W. Ellingsen, Q. Pan and A. H. Strømman, *Materials*, 2019, **12**, 1–14.
- 39 R. Arvidsson, M. L. Söderman, B. A. Sandén, A. Nordelöf, H. André and A. M. Tillman, *Int. J. Life Cycle Assess.*, 2020, **25**, 1805–1817.
- 40 P. Johansson, S. Alvi, P. Ghorbanzade, M. Karlsmo, L. Loaiza, V. Thangavel, K. Westman and F. Åréen, *Batteries Supercaps*, 2021, **4**, 1785–1788.
- 41 R. E. Ciez and D. Steingart, *Joule*, 2020, **4**, 597–614.
- 42 G. A. Elia, G. Greco, P. H. Kamm, F. García-Moreno, S. Raoux and R. Hahn, *Adv. Funct. Mater.*, 2020, **30**, 2003913.
- 43 K. V. Kravchyk and M. V. Kovalenko, *Adv. Energy Mater.*, 2019, **9**, 1901749.

44 M. Chordia, A. Nordelöf and L. A. W. Ellingsen, *Int. J. Life Cycle Assess.*, 2021, **26**, 2024–2039.

45 J. F. Peters, M. Baumann, J. R. Binder and M. Weil, *Sustainable Energy Fuels*, 2021, 6414–6429.

46 K. V. Kravchyk, C. Seno and M. V. Kovalenko, *ACS Energy Lett.*, 2020, 545–549.

47 J. Zheng, D. C. Bock, T. Tang, Q. Zhao, J. Yin, K. R. Tallman, G. Wheeler, X. Liu, Y. Deng, S. Jin, A. C. Marschilok, E. S. Takeuchi, K. J. Takeuchi and L. A. Archer, *Nat. Energy*, 2021, **6**, 398–406.

48 T. Mandai and P. Johansson, *J. Mater. Chem. A*, 2015, **3**, 12230–12239.

49 X. G. Yang, T. Liu and C. Y. Wang, *Nat. Energy*, 2021, **6**, 176–185.

50 Z. Song, Y. Qian, T. Zhang, M. Otani and H. Zhou, *Adv. Sci.*, 2015, **2**, 1–9.

51 S. Wang, K. V. Kravchyk, A. N. Filippin, U. Müller, A. N. Tiwari, S. Buecheler, M. I. Bodnarchuk and M. V. Kovalenko, *Adv. Sci.*, 2018, **5**, 1700712.

52 B. Westlake, Recycling and Disposal of Battery-Based Grid Energy Storage Systems: A Preliminary Investigation, EPRI, Palo Alto, CA, 2017, 3002006911.

53 ABB White Paper: Utility-scale battery energy storage system (BESS) - BESS 4.0 MWh system design, p. 2021.

54 V. Dieterich, J. D. Milshtein, J. L. Barton, T. J. Carney, R. M. Darling and F. R. Brushett, *Transl. Mater. Res.*, 2018, **5**, 034001.

55 D. T. Cuskelly, E. H. Kisi and H. O. Sugo, *J. Solid State Chem.*, 2016, **233**, 150–157.

56 S. Weber, J. F. Peters, M. Baumann and M. Weil, *Environ. Sci. Technol.*, 2018, **52**, 10864–10873.

57 N. Susarla and S. Ahmed, Estimating the cost and energy demand of producing lithium manganese oxide for Li-ion batteries, United States: N. p., 2020, DOI: [10.2172/1607686](https://doi.org/10.2172/1607686).

58 A. Merlo and G. Léonard, *Materials*, 2021, **14**, 3823.

59 V. Ramasamy, D. Feldman, J. Desai and R. Margolis, U.S. Solar Photovoltaic System and Energy Storage Cost Benchmarks: Q1 2021, National Renewable Energy Laboratory, NREL/TP-7A40-80694, 2021, <https://www.nrel.gov/docs/fy22osti/80694.pdf>.

60 L. V. Thomas, O. Schmidt, A. Gambhir, S. Few and I. Staffell, *J. Energy Storage*, 2020, **28**, 101230.

61 M. Iturrrondobeitia, O. Akizu-Gardoki, O. Amondarain, R. Minguez and E. Lizundia, *Adv. Sustainable Syst.*, 2022, **6**, 2100308.

62 S. Middlemas, Z. Fang and P. Fan, *J. Cleaner Prod.*, 2014, 1–11.

63 C. Spanos, D. E. Turney and V. Fthenakis, *Renewable Sustainable Energy Rev.*, 2015, **43**, 478–494.

64 S. Righi, A. Morfino, P. Galletti, C. Samorì, A. Tugnoli and C. Stramigioli, *Green Chem.*, 2011, **13**, 367–375.

65 A. Nordelöf, M. Alatalo and M. L. Söderman, *Int. J. Life Cycle Assess.*, 2019, **24**, 78–92.

